A molecular dynamics study of the sputtering of the W(100) surface by low-energy He, Ar and Kr ions

A molecular dynamics study of the sputtering of the W(100) surface by low-energy He, Ar and Kr ions

Andris Azens, Gundars Romanovskis and Uldis Kanders

Institute of Solid State Physics, Latvian University, 8 Kengaraga Street, Riga 226063, Latvia

Abstract. The sputtering of a tungsten (100) surface by bombardment with 400 eV He, Ar and Kr ions has been investigated by a molecular dynamics simulation. The model is described in detail. It is found that direct ejection by ions contributes significantly to the total sputtering yield for all the ions considered. The characteristics of sputtered atoms and reflected ions are presented. It is revealed by the simulation that the energy distributions of sputtered atoms depend on the sputtering mechanisms and therefore on the primary-ion type. The angular distributions are determined by the surface structure and are similar for He, Ar and Kr.

1. Introduction

The sputtering of solid surfaces by low-energy (hundreds of electronvolts to 20 keV) ion beams has been extensively studied because of wide applications in thin-film technology and surface analysis. Molecular dynamics (MD) computer simulation is a well established method for theoretical investigation of ion–surface interactions and sputtering [1]. The main advantage of the method is the possibility of following the sequence of events on an atomic scale. This makes MD simulations attractive for detailed study of the microscopic mechanisms of sputtering, diffusion, radiation damage, thin-film growth, etc.

The majority of the simulations of sputtering and radiation damage have been performed on FCC materials, mainly Cu and Ag (see, e.g. [2–6]). Tungsten is a representative of heavy elements with a large difference between the incident ion and target atom masses. Therefore one can expect some specific features of sputtering, which is unusual with relatively light elements. We have carried out the MD simulation of the sputtering of a tungsten (100) surface with 400 eV He, Ar and Kr ions. The aim of the present work is to examine the ejection mechanisms of tungsten atoms and their dependence on primary-ion type.

2. Description of the model

2.1. W structure and interatomic potentials

Solid tungsten is represented by the finite-size crystallite (11 atoms × 11 atoms × 5 atoms; BCC lattice; $d_W = 3.16$ Å). The main demand on the crystal size in MD simulations is due to the size of collision cascades. Although the crystal of 11 atoms

× 11 atoms × 5 atoms fails to contain all the cascades completely, the number of ejected particles is not altered by further increasing the number of atoms per layer or the number of layers. With such a size and a 400 eV primary-ion energy there are some high-energy tungsten atoms escaping through the bottom and some low-energy particles leaving the crystal through the other faces. The former move in directions nearly perpendicular to the surface, having almost no chance of reversing the impulse backwards. The latter have insufficient energy to deliver it until the surface is reached, and cause sputtering. For comparison, a Rh crystallite of five layers and with 108 atoms per layer is used to simulate the sputtering by 3 keV argon ions in [7].

One of the basic problems in MD simulations is the selection of interatomic potentials. The physical origin of the atomic interactions is of a many-body and quantum mechanical nature; adequate description of these interactions is one of the most difficult problems in condensed-matter physics. It has proved possible to use empirical pairwise potentials to investigate collision cascade dynamics and sputtering subsequent to the ion impact at a semiquantitative level [3, 8]. In particular, for energy and angular distributions of sputtered atoms, reasonable agreement with experiment is obtained [7, 9]. To study specific quantitative aspects of sputtering, even purely repulsive potentials have been used (see, e.g. [4, 10]). In the present simulation the Johnson–White (JW) potential [11] is employed to describe the tungsten–tungsten interaction. This potential is derived for tungsten on the basis of the elastic constants,   ₌ cohesive energy, vacancy formation energy and lattice constant; satisfactory agreement between phonon dispersion curves predicted by the JW potential and observed experimentally is obtained [11]. As the JW potential is applicable in the vicinity of the equilibrium positions, the Molière potential is used to describe the repulsion of atoms at short separation distances. (This is a common approach; see, e.g., [12, 13].) Thus, the interaction of two tungsten atoms at a separation r is described by the potential $U_W(r)$:

$$U_W(r) = \begin{cases} 0 & r > 3.8 \text{ Å} \\ \text{JW} & 2.5 \text{ Å} \leqslant r \leqslant 3.8 \text{ Å} \\ \text{cubic spline} & 2.3 \text{ Å} < r < 2.5 \text{ Å} \\ \text{Molière} & r \leqslant 2.3 \text{ Å} \end{cases}$$

The JW potential reaches zero at $r = 3.8$ Å, and no artificial cut-off is made in the model. For the (100) surface the JW potential yields normal relaxation of two monolayers. The first layer is shifted outwards for $0.030d_W$, and the second inwards for $0.011d_W$, compared with the position in the bulk. Comparison of theoretical and experimentally observable relaxation of surface layers should be useful to check the validity of the potentials employed. At present, experimental information about the surface structure of tungsten is rather limited. It is concluded from LEED data that 'models with pure vertical displacements of surface atoms can be clearly ruled out' [14]. On the other hand, only a vertical shift for approximately 0.1 Å of the topmost layer is reported in [15] (also from LEED). One can conclude that the surface relaxation predicted by the JW potential differs from experimental data no more than the experimental results reported by different workers. Therefore it appears reasonable to use this potential for MD simulations of sputtering of tungsten.

As the JW potential yields a relaxed surface structure, no additional forces are required to ensure stability. The structure of other faces of the crystallite is that of the bulk. Also the atoms on these faces are not supplied with extra forces. Although

there are some uncompensated forces arising from a lack of neighbouring atoms, no relaxation of boundary faces takes place during the simulation due to employment of the moving-atom approximation (see section 2.3).

The Molière potential is often used to describe the ion–atom interaction [7, 12, 16], in particular in the case of the Ar ion–Mo crystal interaction. Also in the current model the Molière potential is assumed for the ion–tungsten interaction. The potential cut-off is made at a value of 0.5 eV (2.3 Å, 2.7 Å and 2.73 Å for He, Ar and Kr, respectively).

2.2. Simulation of atomic motion

At the very beginning of the simulation, tungsten atoms are placed at equilibrium positions and have zero velocities. Ions with the initial kinetic energy (400 eV) are aimed normally at the fresh surface from the ion–tungsten potential cut-off distance. Atomic collisions are assumed to be elastic; thermal vibrations are not taken into account. The velocity form of the Verlet algorithm [17] is used to calculate the positions and velocities of the particles. This algorithm has proved to be numerically stable even with relatively large time steps [18]. Simulation follows the general scheme

$$Q_i(t), V_i(t) \rightarrow F_i(t) \rightarrow Q_i(t + \Delta t), V_i(t + \Delta t). \tag{1}$$

Q, V and F are coordinates, velocities and forces, respectively; i denotes the atom number. Cycle (1) constitutes one computational step. Such steps are repeated until the total energy of the most energetic particle in the crystallite falls below the zero. Typically the development of collision cascade lasts 100–300 fs, taking 15 000–40 000 computational steps.

105 ion impacts are performed within the representation triangle to take into account the ion–surface interaction dependence on impingement position (points in the triangle would be representative of any point in the surface plane). To check the dependence of the results on the number of incident particles, a run with 210 argon primary ions is performed. The conclusions of the current work are not affected by improved statistics; the main consequence is the smoothing of energy and angular distribution curves. Additional simulation of 30 Ar ion impacts at selected surface points is carried out to test the validity of the moving-atom approximation (see section 2.3).

2.2.1. *The moving-atom approximation.* To save computing time the forces $F_i(t)$ in the current computational step are calculated only for particles with kinetic energy above the threshold $E_m = 1$ eV (these particles are termed 'moving'). Coordinates and velocities are calculated for particles affected by the non-zero force, i.e. for 'moving' atoms and their 'non-moving' neighbours. While the energy of such a neighbour is below E_m, it moves as a free particle exclusively under the influence of the 'moving' atom. Some error can possibly arise from paying no regard to the other surrounding ('non-moving') atoms at the early stage of motion of every particle. It seems reasonable to compare the range of excess motion due to the moving-atom approximation with thermal vibration amplitude. If the value of 1 eV is taken for E_m, the approximation has caused artificial motion for about $3 \times 10^{-4} d_W$ at the moment when the atom becomes 'moving' (compared with the case of when $E_m = 0$). This value is much less than the thermal vibration amplitude at room temperature.

Table 1. Characteristics of sputtered tungsten atoms: sputtering yield Y_W; fraction of energy E_W carried away by the flux of sputtered atoms (in percentage of the total energy supplied by the flux of primary ions); contribution of different ejection mechanisms (primary recoils (i.e. atoms struck by primary ions), secondary recoils (i.e. atoms struck by primary recoils) and cascades) to the sputtering yield (in percentages); contribution of surface layers to the sputtering yield (in percentages).

			Contribution of different W ejection mechanisms			Contribution from the following layers of W origin	
Ion	Y_W	E_W	Primary recoils	Secondary recoils	Cascades	1	2
He	0.07	0.2	88.8	5.6	5.6	100	
Ar	0.9	7.6	47.6	25.3	27.1	97.5	2.5
Kr	1.4	8.1	16.4	18.2	65.4	97.0	3.0

To test the approximation, the simulation of 30 argon ion impacts has been performed at selected surface points, yielding more than 50% of all sputtered particles. The value of $E_m = 0.1$ eV was chosen for this case. The number of ejected particles was not affected by a reduction in E_m. The difference between the energies of sputtered atoms was in the range 0.05–0.3 eV, compared with the case when $E_m = 1$ eV.

The moving-atom approximation is similar to that used in [12], where it has already been concluded that the loss of weak interaction between the atoms is admissible within the model. The main difference is that in our model the 'moving' atom interacts with all its neighbours, while some force threshold is used to account for such interaction in the model of [12]. As a result, extra energy is retained by the 'moving' atom in [12]. In contrast, the amount of energy transferred to the 'non-moving' neighbours is slightly overestimated in the present simulation.

2.2.2. Choice of the time step Δt. Much computing time is required if a constant time step is used in the model. When the energy of the primary ion is dissipated between the atoms of the solid, there are many slowly moving particles instead of one rapidly moving particle. If Δt is not increased, many computational steps have to be carried out to simulate the motion of these low-energy atoms. In the current simulation the time step Δt is overcalculated in each computational step as

$$\Delta t = \left\{ -V_n(t) + [V_n^2(t) + 2CU_{nt}(t)/m_n]^{1/2} \right\} m_n/F_n(t). \qquad (2)$$

n denotes the number of the most energetic particle anywhere in the system; m_n and U_{nt} are the mass and the total energy of the nth particle, respectively. C represents the ratio $C = \Delta U_{np}/U_{nt}$ where ΔU_{np} is the change in potential of the nth particle during Δt. C is taken to be constant for the duration of the simulation. Calculating Δt from (2) the potential of the most energetic particle is allowed to vary by a constant fraction (equal to C) of its total energy in each step. The value $C = 1/1200$ is used in the present calculations.

3. Results and discussion

The characteristics of sputtered W atoms are summarized in table 1, and the characteristics of reflected ions in table 2.

The main trends revealed by the simulation are the following.

Ion	R_i	E_i	Reflected ions			Back-scattering ions reflected by the following number of layers		
			$N_{iW} = 1$	$N_{iW} = 2$	$N_{iW} > 2$	1	2	3
He	0.11	19.2	29.6	19.4	51.0	20.9	59.7	13.2
Ar	0.49	27.7	9.9	13.8	76.3	23.3	55.5	16.7
Kr	0.60	20.7	9.6	10.1	80.3	19.6	64.8	15.6

(i) The vast majority of sputtered atoms originate from the first surface layer.

(ii) Ejection directly by ions plays a significant role in the sputtering of tungsten. Primary recoils constitute nearly all the sputtered flux in the case of He and about half in the case of Ar. Even in the case of Kr, 16% of W atoms are ejected by ions. This feature is indirectly confirmed by experimental results on the sputtering of chemisorbed nitrogen from W(100) [19]. It is concluded in [19] that direct collisions make a significant contribution to the nitrogen sputter yield (approximately 80% at 500 eV Ar energy). If sputtering by collision cascades was dominant in the case of metallic tungsten, it would also be responsible for the ejection of chemisorbed species.

(iii) Collisions along the close-packed directions determine the angular distribution of the sputtered particles and also affect the atoms ejected directly by ions.

(iv) In all cases the flux of sputtered atoms possesses less than 10% of the total energy, supplied by primary ions.

(v) The total energy retained by the reflected ions exceeds the total energy of the sputtered atoms by several times.

(vi) Only a minority of the reflected ions are back-scattered by the first atomic layer or by a single ion–atom collision.

In general, the sputtering mechanism is determined by the ion mass and size and by the crystal structure. A small ion mass compared with the mass of tungsten leads to restricted energy transfer from ion to any tungsten atom in a single collision and is insufficient for the development of a collision cascade in the crystal. On the other hand, the ion is not stopped after one or two collisions. That is why direct ejection by ions prevails in the case of light ions. The ion size together with the crystal structure determine the motion of ions within the solid. The extremely low sputtering and reflection yields for helium are caused by channelling of He through the crystal. Most He ions pass through five layers of tungsten atoms, neither significantly losing energy nor changing the velocity direction. From this viewpoint one of the reasons for the unexpectedly high sputtering yields reported for molecular ions (see, e.g., [20]) should be the large ion size, preventing the penetration of the ion deep into the solid and promoting the dissipation of energy in a thin near-surface layer.

The energy distributions of sputtered tungsten atoms are shown in figure 1. The distribution in the case of Kr peaks at a higher energy compared with that for Ar. Deviation from this sequence for He is caused by the sputtering of tungsten atoms directly by He ions. Also, of the atoms sputtered by bombardment with Ar and Kr, primary recoils possess higher energies than particles originating from
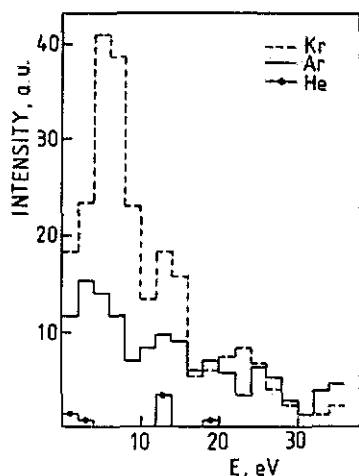
Figure 1. Energy distributions of tungsten atoms sputtered by bombardment with He, Ar and Kr ions.
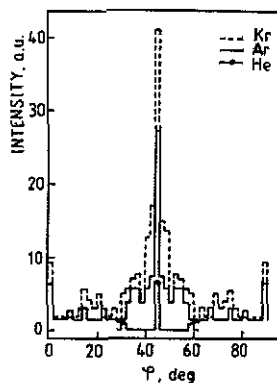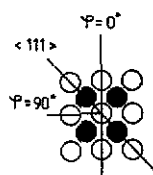

Figure 2. Azimuthal angle distributions of tungsten atoms sputtered by bombardment with He, Ar and Kr ions. The distributions are integrated over all polar angles. The coordinate system is shown on the left-hand side. The open circles represent the top-layer atoms and the full circles represent the second-layer atoms.

collision cascades. Generally, the greater the contribution of sputtering directly by ions, the more the energy plot differs from the dependence $1/E^2$ predicted for cascade sputtering by analytical theories [21].

The angular distributions of sputtered atoms are shown in figures 2 and 3. The main maxima in both polar and azimuthal distributions are related to the close-packed direction $\langle 111 \rangle$. There is no tangential shift of surface atom layers, and there are sharp maxima in azimuthal distributions. The main peak corresponds to the azimuth of direction $\langle 111 \rangle$ (see figure 2). The azimuthal directions of sputtered atoms are not affected by vertical shifts of surface layers. This is quite natural, because the angles between atoms in the plane shown in figure 2 do not depend on the distance between the layers. The sharpness of the peaks of azimuthal distributions reflects the effects of marked focusing by the crystal lattice.

The surface atoms in figure 3 are not placed on a straight line in direction $\langle 111 \rangle$ owing to the vertical shifts of surface layers. As a result, collision chains in this direction are defocused (non-central collisions take place in the plane of figure 3) and the main peak position in the polar distribution does not correspond either to a polar angle of direction $\langle 111 \rangle$ (θ_1) or to that of θ_s in figure 3. It should be noted that the peak position (about 38°) differs more from θ_1 than θ_s does. The pronounced dependence of peak position on layer shifts is consistent with results of [9], where it is found that two random monolayers on a crystalline Cu target 'nearly destroy the angular distributions due to the underlying structure'.

Although the model describes the sputtering coefficient dependence on primary-ion type with reasonable accuracy (figure 4), absolute yields are larger than experimental: 0.04, 0.4 and 0.6 for He, Ar and Kr, respectively [22]. The sputtering yield is more sensitive to the choice of model parameters than are the distribution functions [23, 24]. As the possible reasons for the yield overestimation, usually the choice
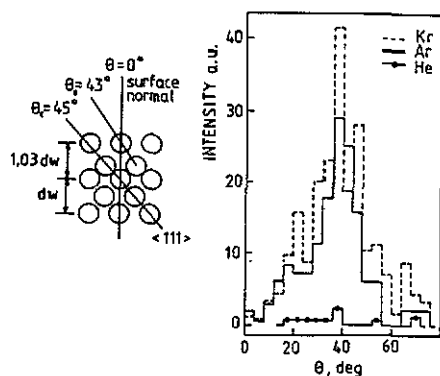
Figure 3. Polar angle distributions of tungsten atoms sputtered by bombardment with He, Ar and Kr ions. The distributions are integrated over all azimuthal angles. The coordinate system is shown on the left-hand side.
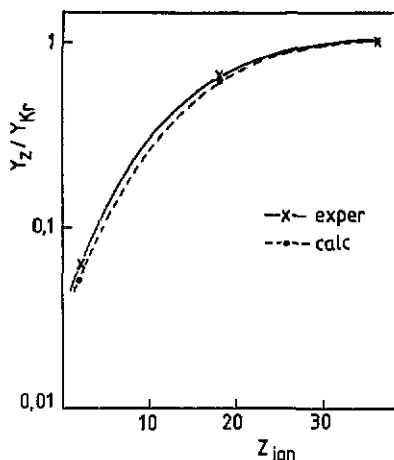
Figure 4. Dependence of the sputtering yield of tungsten on primary-ion type. Yields are normalized to that of Kr. Experimental values are from [22].

of interatomic potentials and neglect of inelastic energy losses are considered. The latter effect seems to be of minor importance in the present situation. First of all, 400 eV is too low an energy for inelastic losses to play a role [25]. Introduction of inelastic losses in the simulation of sputtering of Cu by 5 keV Ar ions decreased the sputtering yield by 15% [10]; in the case of 400 eV, one can expect a much smaller value. Further, in the present simulation, collision cascades are developed to an insufficient extent to lose the energy due to the electronic stopping, even if the stopping power is considerable. Apparently there must be another reason for the discrepancy in the sputtering yield. The atom–atom and ion–atom potentials are found to affect the sputtering yield markedly [23, 24]. Following the ideas of [23, 24], one has to decrease the size of particles to reduce the calculated yield. However, we have not varied the potential functions in this work. Our opinion is that the present degree of sophistication is sufficient to indicate the basic features of the sputtering phenomenon. Besides this, there could also be other reasons for the yield discrepancy. In particular, the assumption of a fresh surface should lead to an overestimation of the number of sputtered particles. Experimental yields are almost never measured from perfect surfaces. Damaged surface layers can affect the focused energy transfer by destroying the propagation of collision chains in close-packed directions. As the effect of the surrounding lattice is revealed to be significant, the measured sputtering yield should depend upon the primary-ion dose. It is worth mentioning that also the analytical theory overestimates the yield of tungsten by a factor of $\simeq 3$ [22].

As the current model fails to describe the sputtering coefficient, the concrete percentage of different sputtering mechanism contributions to the total yield should also be treated with some caution. Nevertheless the conclusion about the importance of sputtering directly by ions remains valid, because the difference in the masses and characteristic sizes (the size of the ion compared with the open space in crystal) must play a role in every reasonable set of model parameters.

4. Conclusions

Ejection directly by ions makes a significant contribution to the sputtering of the (100) tungsten surface by bombardment with 400 eV He, Ar and even Kr ions.

The energy distributions of ejected tungsten atoms depend on the mechanisms involved in the sputtering. The primary recoils possess higher energies than the atoms sputtered by the collision cascades. The contributions of direct ion and cascade sputtering differ for He, Ar and Kr ions, making the energy distributions of the sputtered atoms dependent on the primary-ion type.

Angular distributions of the sputtered atoms are determined by the surface structure and are similar in the cases of He, Ar and Kr. Even small shifts of the surface layers can destroy the focused collision chains and affect significantly the peak positions in angular distributions. From the viewpoint of model development the utilization of a highly suitable interatomic potential, responsible for the surface structure, is crucial for reliable results.

References

[1] Harrison D E 1988 *Crit. Rev. Solid State Mater. Sci.* 14 S1–78
[2] Gibson J B *et al* 1960 *Phys. Rev.* 120 1229–53
[3] Garrison B J, Winograd N and Harrison D E 1978 *J. Chem. Phys.* 69 1440–4
[4] Hautala M and Likonen J 1988 *Nucl. Instrum. Methods* B 33 526–9
[5] Harrison D E *et al* 1978 *Surf. Sci.* 76 311–22
[6] Chou S P and Ghoniem N M 1991 *Phys. Rev.* B 43 2490–5
[7] Garrison B J *et al* 1987 *Phys. Rev.* B 36 3516–21
[8] Jakas M M and Harrison D E 1985 *Phys. Rev. Lett.* 55 1782–5
[9] Reimann C T *et al* 1988 *J. Chem. Phys.* 89 2539–43
[10] Likonen J and Hautala M 1989 *J. Phys.: Condens. Matter* 1 4697–722
[11] Johnson R A and White P J 1976 *Phys. Rev.* B 13 5293–302
[12] Smith R, Harrison D E and Garrison B J 1989 *Phys. Rev.* B 40 93–101
[13] Garrison B J *et al* 1988 *Phys. Rev.* B 37 7197–204
[14] Landskron H *et al* 1989 *J. Phys.: Condens. Matter* 1 1–12
[15] Van Hove M A and Tong S Y 1976 *Surf. Sci.* 54 91–100
[16] Chakarov I R *et al* 1989 *Nucl. Instrum. Methods* B 39 81–5
[17] Gould H and Tobochnik J 1988 *An Introduction to Computer Simulation Methods Applications to Physical Systems* (Reading, MA: Addison-Wesley)
[18] Brandt E H 1989 *J. Phys.: Condens. Matter* 1 9985–10 001
[19] Winters H F and Taglauer E 1987 *Phys. Rev.* B 35 2174–87
[20] Thompson D A and Johar S S 1981 *Radiat. Eff.* 55 91–8
[21] Sigmund P 1969 *Phys. Rev.* 184 383–416
[22] Andersen H H and Bay H L 1981 *Sputtering by Particle Bombardment* ed R Berish (Berlin: Springer)
[23] Harrison D E 1981 *J. Appl. Phys.* 52 1499–508
[24] Harrison D E and Webb R P 1982 *J. Appl. Phys.* 53 4193–201
[25] Feldman L C and Mayer J W 1986 *Fundamentals of Surface and Thin Film Analysis* (Amsterdam: North-Holland)